ARKIV FÖR FYSIK Band 13 nr 17

Communicated 11 September 1957 by O. Klein and I. Waller

On the scattering of slow neutrons by KCl

By Alf Sjölander

With 10 figures in the text

ABSTRACT

Numerical calculations of the coherent and incoherent one-phonon scattering of slow neutrons by a single KCl crystal are presented. The one-phonon scattering surfaces for a series of neutron energies and some different crystal settings have been determined on the basis of the eigen frequencies obtained by Tenerz when using a realistic model of KCl. Rough estimates of the scattering intensities have also been made.

I. Introduction

In 1938 and 1942 Pomeranchuk [1] and Seeger and Teller [2] discussed certain features of the inelastic scattering of thermal neutrons against crystals. Since then many authors have developed the theory in more detail. Especially two of them, Placzek and Van Hove [3], have emphasized that processes where only one vibration quantum participates would give valuable information on the crystal vibrations. In such cases measurements of the relation between the energies of the scattered neutrons and the scattering angle would give the frequencies for any single vibration wave vector, at least in principle. To make sure that multi-phonon processes do not disturb the measurements the energy of the incoming neutrons and the temperature must not be too high. In recent years some successful experiments have been performed to measure this energy exchange corresponding to one-phonon processes [4–10].[1]

Squires [11] has made a calculation of the energy-angle relation for aluminium based on the Born-von Karmàn model for the crystal vibrations. The present paper contains a presentation of similar calculations for KCl at room temperature and a rough estimate of the intensity of the scattered neutrons is made. The eigen frequencies were determined by Tenerz [12] in connection with a study of the specific heat. The crystal was then considered a simple cubic one. In some respects these calculations seem to be more reliable than a previous one by Iona, owing to the fact that the actual charge of the ions has been replaced by the effective charge, in agreement with experiments [13]. The short range forces were determined from the experimental data of the elastic constants and the residual ray frequency. Subsequently new calculations were made using a more detailed model and these results ought to be more trustworthy [14].[2]

---

[1] Dr. Larsson and collaborators at the Swedish Atomic Energy Company have also recently performed such experiments, with very good energy resolution.

[2] When the calculations presented in this paper were performed (1955) only the earlier results on the eigen frequencies were available. There are fairly large discrepancies between these and the later ones, not yet published, and therefore the numerical results in this paper must be taken only as a rather crude approximation for KCl.

II. The eigen vibrations of the crystal

In the calculation of the frequencies mentioned above the K+- and Cl−-ions were considered identical, apart from their charges, and a cubic reciprocal units cell with edge length $2\pi/a$ was introduced, a being the distance between the nearest ions (a K+- and a Cl−-ion). The frequencies and the polarization vectors of the vibrations were determined from a system of equations

$$\omega^2 C_x = \sum_y D_{xy} C_x \tag{1}$$

where the dynamical tensor D_{xy} depends on the wave vector $\mathbf{q}$. For each $\mathbf{q}$ there are three different modes of vibration, characterized by

$$\omega_j(\mathbf{q}) \text{ and } \mathbf{C}_j(\mathbf{q}), \quad j=1,2,3.$$

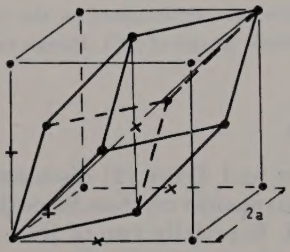

Fig. 1. The direct unit cell;
● K-atom, × Cl-atom.

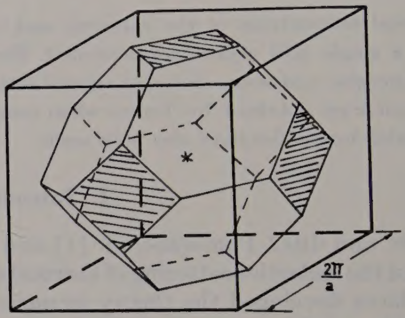

Fig. 2. The reciprocal unit cell.

Two of these correspond to "transversal vibrations" and one corresponds to a "longitudinal vibration".[1]

The K and Cl nuclei scatter neutrons differently and therefore it would in our case be more convenient to consider the crystal as a face-centered cubic lattice (the unit cell is drawn in Fig. 1) occupied by a K+-ion at the lattice points and a Cl−-ion in the middle of each unit cell. The corresponding reciprocal lattice is then a body-centered cubic one. Its unit cell, the first Brillouin zone, is drawn in Fig. 2, within the cubic reciprocal cell above.[2]

The eigen vibrations are then determined from the following altered system of equations

$$\omega^2 C_x^k = \sum_{k',y} D_{xy}^{kk'} C_y^{k'} \quad k, k' = 1, 2 \tag{2}$$

$k=1$ refers to a K$^+$-ion
$k=2$,, ,, ,, Cl$^-$-ion

and normalized according to $\sum_k |\mathbf{C}^k|^2 = 1$. For each $\mathbf{q}$ there are now six modes of vibration, three acoustic ones and three optical ones, with their characteristic quantities

$$\omega_j(\mathbf{q}), \quad \mathbf{C}_j^1(\mathbf{q}), \quad \mathbf{C}_j^2(\mathbf{q}), \quad j=1, 2, \ldots, 6.$$

---

[1] The polarization vectors are exactly parallel and perpendicular to the wave vector only for certain symmetry directions of $\mathbf{q}$.

[2] Note that a factor of 2π is included in our definition of the reciprocal lattice.

We note, however, that in this case the wave vectors fill a smaller volume than above (see Fig. 2).

To use the numerical results by Tenerz we must identify the solutions from (1) and (2) respectively. Thus the three acoustic solutions of eqs. (2) correspond to the three solutions of eqs. (1) with the same wave vector and eigen frequencies. The relation between the polarization vectors is

$$\mathbf{C}_j^k(\mathbf{q}) = \mathbf{C}_j(\mathbf{q})\, e^{i\mathbf{q}\cdot\mathbf{r}_k}, \quad j = 1, 2, 3 \tag{3'}$$

where $\mathbf{C}_j(\mathbf{q})$ refers to the representation in (1) and $\mathbf{r}_k$ are the position vectors of the ions in the zero unit cell.[1] The optical branches in (2) on the other hand correspond to the solutions of (1) for a wave vector $\mathbf{q}'$ outside the polyhedron. The frequencies and polarization vectors of the optical branches are determined from

$$\begin{aligned} &\omega_j(\mathbf{q}) = \omega_{j'}(\mathbf{q}'), \quad \mathbf{C}_j^k(\mathbf{q}) = \varepsilon_k \mathbf{C}_{j'}(\mathbf{q}')\, e^{i\mathbf{q}\cdot\mathbf{r}_k} \\ &\varepsilon_1 = 1, \quad \varepsilon_2 = -1, \quad j = 4, 5, 6, \quad j' = 1, 2, 3 \end{aligned} \tag{3''}$$

where $\mathbf{q}' = \mathbf{q} + \boldsymbol{\tau}$, $\boldsymbol{\tau}$ being a certain reciprocal lattice vector.

III. The scattering surfaces

The relation between the energy exchange and the scattering angle is determined from an energy-momentum law [1] (see Fig. 3).

$$\boxed{\begin{aligned} &k^2 = k_0^2 - \varepsilon \frac{2\,m}{\hbar}\,\omega_j(\mathbf{q}) \\ &\mathbf{k} = \mathbf{k}_0 + \mathbf{q} - \boldsymbol{\tau} \end{aligned}} \quad j = 1, 2, 3. \tag{4}$$

Here $\mathbf{k}_0$ = wave vector of the incident neutron.
$\mathbf{k}$ = wave vector of the scattered neutron.
$\boldsymbol{\tau}$ = reciprocal lattice vector, indicating Laue intensity maxima.
ε = ±1, depending on whether neutrons lose or gain energy in the scattering.
m = mass of the neutron.

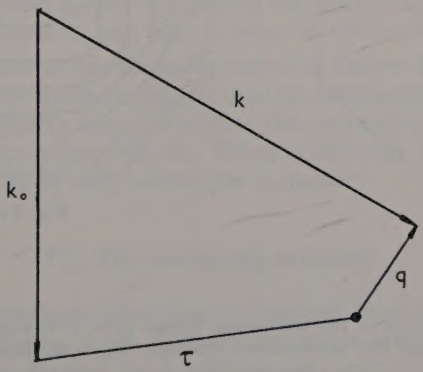

Fig. 3.

---

[1] $\mathbf{r}_1 = a(0,0,0)$, $\mathbf{r}_2 = a(1,1,1)$, where (1,0,0), (0,1,0) and (0,0,1) denote the unit vectors along the principal axis of the crystal.

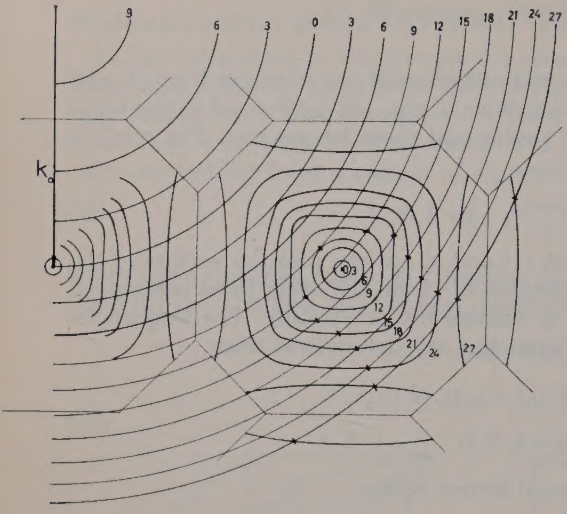

Fig. 4 a.

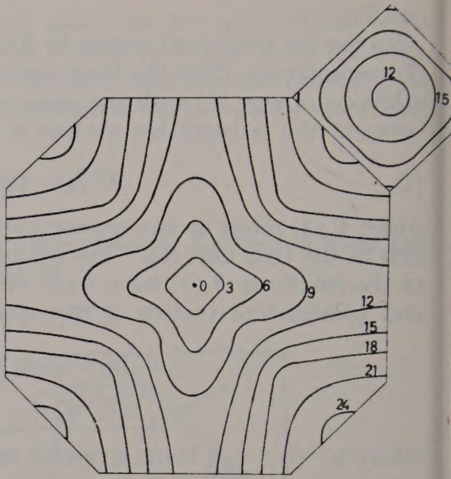

Fig. 4 b.

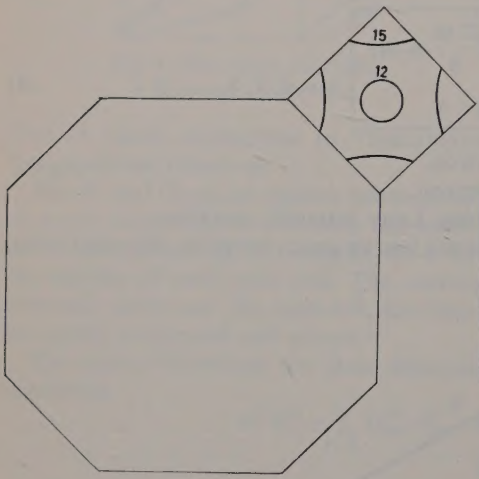

Fig. 4 c.

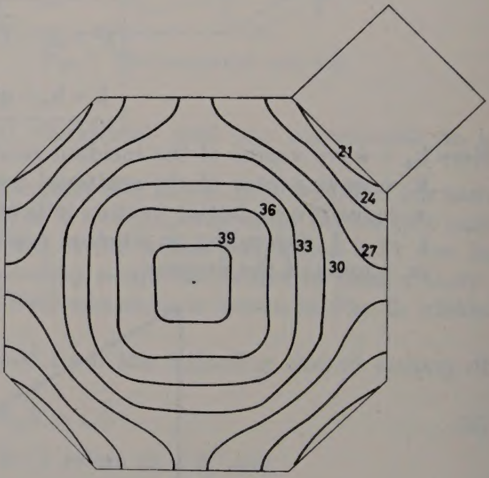

Fig. 4 d.

Fig. 4 a–f. Iso-frequency curves in the scattering plane. (The frequencies are arranged in such a way that the polarization vectors vary continuously.)

a) Acoustic longitudinal branch.
b) First acoustic transversal branch.
c) Second acoustic transversal branch.
d) Optical longitudinal branch.
e) First optical transversal branch.
f) Second optical transversal branch.

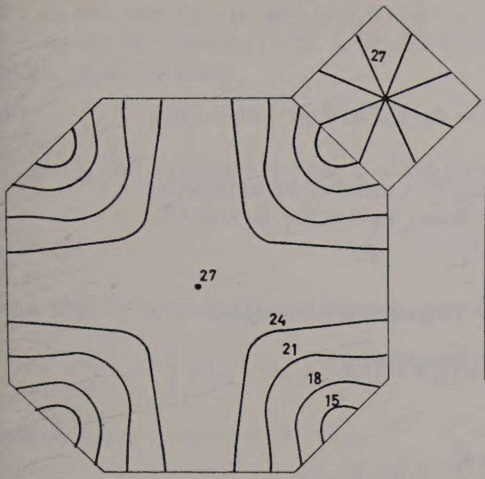

Fig. 4 e.

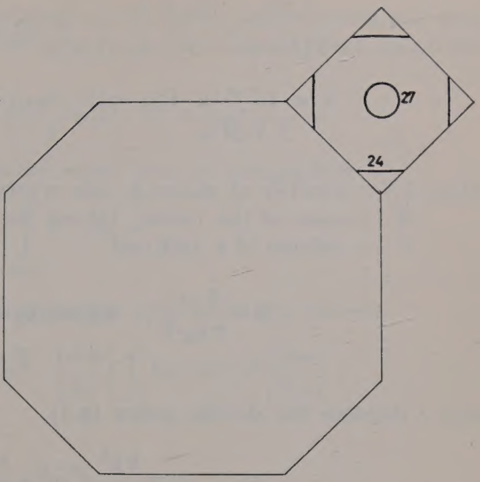

Fig. 4 f.

Our main task has been to solve (4) for a given $\mathbf{k}_0$, thus determining k as a function of the scattering angle. The wave vectors of the scattered neutrons then define a certain scattering surface for each j and ε.

In our calculations neutron energies corresponding to $k_0 = 0$, 1.8, 3.0 and $4.0 \cdot 10^8$ cm^{-1} ($\lambda = (2\pi)/k_0 = \infty$, 3.49, 2.09, 1.57 Å) were considered and the scattering plane was supposed to be perpendicular to a principal axis of the crystal. Only those wave vectors $\mathbf{q}$ reaching points in the $(xy0)$- and $(xy, \pm\pi/a)$-planes of the reciprocal unit cell contribute to the scattering (see Figs. 2 and 3).

The equations (4) were solved graphically in the following way.[1] On one sheet was drawn the contour of the reciprocal lattice in the scattering plane and into each cell were put series of iso-frequency curves, one series for each branch j ($\omega = 1, 2, \ldots, 41\ 10^{12}$ sec^{-1}). Some of these iso-frequency curves are shown in Fig. 4. A blank cell indicates that the corresponding scattering has a vanishing intensity. On another sheet of transparent paper was drawn the vector $\mathbf{k}_0$, representing the wave vector of the incident neutron, and also a series of concentric circles with the radii $k = \sqrt{k_0^2 - \varepsilon\, 2m/\hbar\, \omega}$, where ω has the same values as above. The latter sheet is superimposed on the first one as shown in Fig. 4a, and the intersections between corresponding curves on the two sheets then determine the scattering surfaces in accordance with the energy-momentum law (Fig. 3). When a different direction of the incident neutron is required one need only rotate the k-sheet.

IV. The scattering intensity

The intensity of the scattered neutrons is obtained from the following expression for the differential scattering cross section (the cross section per unit solid angle and unit energy interval divided by $\hbar$ and per unit cell) [15]:

---

[1] The same method has also been suggested by A. Herpin, B. Jacrot, J. Phys. Radium, *16*, 35S (1955).

$$\frac{d\,\sigma_{\mathrm{coh}}^{(1)}}{d\,\Omega\,d\,\omega}=\frac{(2\,\pi)^3}{V}\,\frac{k}{k_0}\sum_{k,k'}\sum_{s,\varepsilon}\langle a_k\rangle\,\langle a_{k'}\rangle\,e^{-W_k-W_{k'}}\,e^{i\boldsymbol{\varkappa}\cdot(\mathbf{r}_k-\mathbf{r}_{k'})}$$

$$\frac{\hbar\,(\boldsymbol{\varkappa}\cdot\mathbf{C}_s^{k'})^*\,(\boldsymbol{\varkappa}\cdot\mathbf{C}_s^{k})}{2\,N\,M\,\omega_s}\;\frac{\coth\,(\beta\,\omega_s)+\varepsilon}{2}\;\delta_P\,(\boldsymbol{\varkappa}+\mathbf{q})\,\delta\,(\omega-\omega_0+\varepsilon\,\omega_s). \tag{5}$$

Here $2N$ = number of atoms in the crystal (N = number of unit cells).
M = mass of the nuclei, taking the mean values for K and Cl.
V = volume of a unit cell.

$$\beta=\frac{\hbar\,\omega_s}{2\,k_B\,T},\quad \text{where } k_B=\text{Boltzmann's constant.}$$
$$T=\text{temperature}$$

and s denotes the double index $(\mathbf{q},j)$.

$$\omega=\frac{\hbar\,k^2}{2\,m},\quad \omega_0=\frac{\hbar\,k_0^2}{2\,m},\quad \boldsymbol{\varkappa}=\mathbf{k}_0-\mathbf{k}$$

$\langle a_k\rangle$ are the coherent bound scattering lengths for K and Cl and their values are taken from Bacon [16].

$$\langle a_{\mathrm{K}}\rangle=0.35\cdot10^{-12}\ \mathrm{cm},\quad \langle a_{\mathrm{Cl}}\rangle=0.99\cdot10^{-12}\ \mathrm{cm}.$$

e^{-W_k} are the Debye-Waller factors, which in the Debye approximation are determined from[1]

$$2\,W_1=2\,W_2=2\,W=\frac{\hbar^2\,\varkappa^2}{2\,M\,k_B\,\Theta}\,6\left(\frac{T}{\Theta}\right)^2\int\limits_0^{\Theta/T}\left(\frac{x}{e^x-1}+\frac{x}{2}\right)d\,x \tag{6}$$

and for $\Theta=219°\mathrm{K}$, the Debye temperature of KCl, and $T=293°\mathrm{K}$ this simplifies to

$$2W=2.45\cdot10^{-18}\,|\,\mathbf{k}_0-\mathbf{k}\,|^2.$$

$\delta(\ldots)$ is an ordinary Dirac function and $\delta_P(\boldsymbol{\varkappa})=\sum\limits_{\boldsymbol{\tau}}(\boldsymbol{\varkappa}-\boldsymbol{\tau})$ means a periodic Dirac function, singular at the reciprocal lattice points.

If the polarization vectors are taken from (3′, 3″) and normalized according to (2), the summation over k,k' gives structure factors of the following type

$$F=\sum_k\langle a_k\rangle\,e^{i\boldsymbol{\varkappa}\cdot\mathbf{r}_k}$$

well known from the ordinary Bragg scattering. The value of this factor depends on whether the wave vector $\mathbf{q}$ is drawn from a corner lattice point or a centre lattice point of the body-centered reciprocal lattice and also on whether the eigen vibration considered is an acoustic or an optical one. Thus

$$F=\langle a_{\mathrm{K}}\rangle+\langle a_{\mathrm{Cl}}\rangle,\qquad |F|^2=1.80\cdot10^{-24}\ \mathrm{cm}^2$$

---

[1] See: R. W. James, The Optical Principles of the Diffraction of X-rays, p. 219, London 1948.

for an acoustic branch ($j = 1, 2, 3$) and $\mathfrak{q}$ belonging to a corner lattice point and also for an optical branch ($j = 4, 5, 6$) and $\mathfrak{q}$ belonging to a centre lattice point. In all the other cases we have

$$F = \langle a_{\mathrm{K}} \rangle - \langle a_{\mathrm{Cl}} \rangle, \qquad |F|^2 = 0.41 \cdot 10^{-24} \text{ cm}^2.$$

In (5) the summation over $\mathfrak{q}$ is first transformed into an integration

$$\sum_{\mathfrak{q}} \rightarrow \frac{V N}{(2\pi)^3} \int_{(\text{cell})} \ldots \, d\mathfrak{q}$$

and this is immediately performed. The integration over ω finally follows:

$$\int \delta\,(\omega - \omega_0 + \varepsilon\, \omega_j\, (\mathbf{k} - \mathbf{k}_0))\, d\omega = \left|\frac{d\omega}{dx}\right| \int \delta\,(x)\, dx = \left|\frac{d\omega}{dx}\right|$$

where $x = \omega - \omega_0 + \varepsilon \omega_j (\mathbf{k} - \mathbf{k}_0)$

$$\frac{dx}{d\omega} = 1 + \varepsilon \frac{\mathbf{n} \cdot \mathbf{c}_s}{v}$$

with $\mathbf{n}$ = unit vector along the scattering direction,
v = velocity of the scattered neutron,
$\mathbf{c}_s$ = grad $\omega_j(\mathfrak{q})$ = group velocity of the wave.

A formula convenient for the calculations of the scattering intensity per unit solid angle and per cell is then obtained.[1]

$$\boxed{\frac{d\sigma^{(1)}_{\text{coh}}}{d\Omega} = \frac{k}{k_0} e^{-2W} |F|^2 \frac{\hbar \varkappa^2}{2M} \frac{(\mathbf{e}_\varkappa \cdot \mathbf{C}_s)^2}{\omega_s} \frac{\coth(\beta\omega_s) + \varepsilon}{2} \frac{1}{\left|1 + \varepsilon \dfrac{\mathbf{n} \cdot \mathbf{c}_s}{v}\right|}\,.} \qquad (7)$$

$\mathbf{e}_\varkappa$ is the unit vector along $\boldsymbol{\varkappa}$ and $(\mathfrak{q}, \boldsymbol{\varkappa})$ are determined from eqs. (4). This formula was first derived by Waller and Fröman [17], and they emphasized the significance of the factor $|1 + \varepsilon\, \mathbf{n} \cdot \mathbf{c}_s / v|^{-1}$ for the scattering.

In our calculations one of the acoustic and one of the optical branches have their polarization vectors perpendicular to the scattering plane, thus giving vanishing intensity (see Fig. 4).

To obtain some numerical results on the intensity we must know the polarization directions and the group velocities. Unfortunately it was not possible to get more than a very rough estimate of the group velocities from the numerical material pertaining to the crystal frequencies. Nevertheless the calculated intensities, uncertain within perhaps a factor of two or more, give some valuable information on the scattering.

V. The singular directions

From (7) is seen that the intensity is infinite when the Laue scattering conditions are fulfilled ($\mathfrak{q} = 0$, $\omega_s = 0$), as well as in the case of those scattering directions where $(1 + \varepsilon\, (\mathbf{n} \cdot \mathbf{c}_s)/v)$ vanishes. These singular directions have been studied earlier in more detail under conditions where they occurred for small wave vectors (near Bragg scattering) [17, 18]. Here we will only show how to construct them when the scattering surfaces are known.

---

[1] Note that according to the normalization of the polarization vectors $\mathbf{C}_s^k$ we have $|\mathbf{C}_s|^2 = 1$.

According to the energy-momentum law (4) we have

$$d\mathfrak{q} = d\mathbf{k}, \quad d\omega = \mathbf{v}\cdot d\mathbf{k} = -\,\varepsilon \operatorname{grad} \omega_j(\mathfrak{q})\cdot d\mathfrak{q}$$

when $\mathbf{k}$ (and $\mathfrak{q}$) runs along a definite scattering surface. Thus

$$(\varepsilon\,\mathbf{c}_s + \mathbf{v})\cdot d\mathbf{k} = 0, \quad \mathbf{c}_s = \operatorname{grad} \omega_j(\mathfrak{q})$$

or in another form

$$\varepsilon\,\mathbf{c}_s + \mathbf{v} = \gamma\,\mathbf{n}_s$$

where $\mathbf{n}_s$ is a unit vector normal to the scattering surface and γ is a scalar factor. Multiplying both sides with $1/v\ \mathbf{n}$ ($\mathbf{n}$ = the unit vector along the scattering direction) we get the factor appearing in (7)

$$1 + \varepsilon\,\frac{\mathbf{n}\cdot\mathbf{c}_s}{v} = \frac{1}{v}\,\gamma\,(\mathbf{n}\cdot\mathbf{n}_s)$$

which vanishes only if $\mathbf{k}$ ($\mathbf{k} = k\mathbf{n}$) is a tangent of the scattering surface. The fact that γ may be zero will not change this result.

VI. The incoherent zero- and one-phonon scattering

In addition to the coherent scattering there will be an incoherent one, due to spin dependence of the scattering lengths of the separate nuclei and to isotopic disorder in the crystal. As for the coherent part the incoherent scattering may be divided into zero-phonon, one-phonon etc. scattering, according to the number of vibrational quanta involved. Only the zero-phonon part gives discrete energies of the scattered neutrons (elastic scattering), whereas in the one-phonon processes the scattered neutrons have for all angles a continuous energy spectrum extending from $\hbar(\omega_0 - \omega_m)$ to $\hbar(\omega_0 + \omega_m)$, and analogous for the higher phonon processes. ω_m means the maximum vibrational frequency. In principle it would be possible to distinguish experimentally neutrons scattered in an incoherent zero-phonon and a coherent one-phonon process from those scattered in other processes, using the fact that in the first case the neutrons have discrete energies. However, the detectors have a finite resolving power and this limits the practical use of this distinction. It would therefore in some cases be necessary to correct for these other processes.

The differential scattering cross sections per unit cell are written below for the incoherent zero- and one-phonon processes [19].[1] The two-phonon scattering, especially the coherent one, is discussed in a separate paper [20].

$$\boxed{\begin{aligned} \frac{d\,\sigma^{(0)}_{\text{incoh}}}{d\,\Omega\,d\,\omega} &= A\,e^{-2W}\,\delta(\omega-\omega_0) \\ \frac{d\,\sigma^{(1)}_{\text{incoh}}}{d\,\Omega\,d\,\omega} &= A\,\frac{k}{k_0}\,e^{-2W}\left[\frac{\hbar\,\varkappa^2}{2\,M}\,\gamma\,(0)\right] g\,(\omega-\omega_0) \end{aligned}} \qquad \begin{aligned} &(8) \\ &(9) \end{aligned}$$

---

[1] See also Placzek and Van Hove, loc. cit.

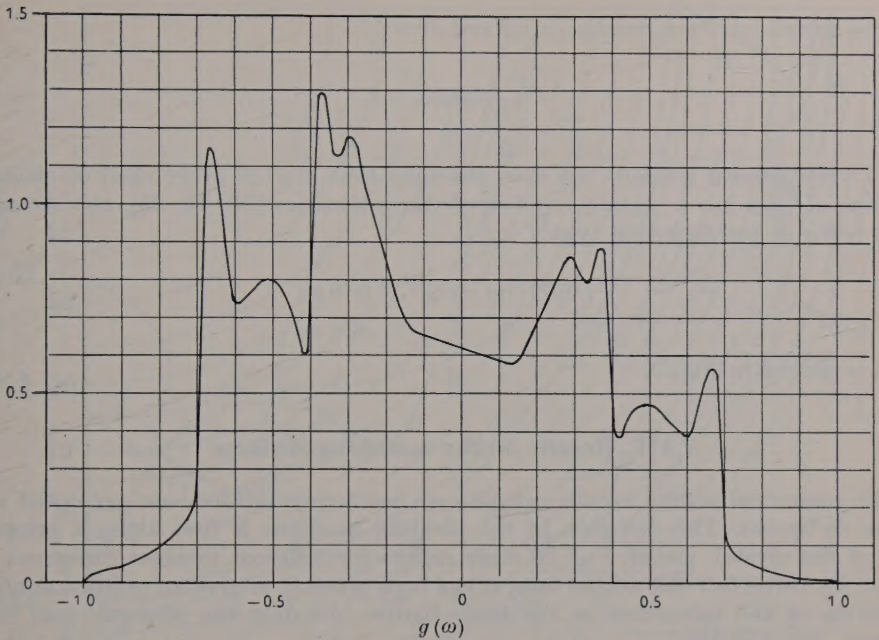

Fig. 5. To get the normalization according to formula (13) the values obtained from the figure must be multiplied by the factor 0.976.

e^{-2W} is, as above, the Debye-Waller factor and A means the sum of the incoherent differential scattering cross section of K and Cl taken for bound nuclei [16].

$$A = 0.26 \cdot 10^{-24}\ \text{cm}^2$$

$g(\omega)$ is defined by

$$\begin{aligned} g(\omega) &= \frac{f(\omega)}{2\,\omega\,\gamma(0)}\left[\coth(\beta\,\omega) - 1\right], & |\omega| \leqslant 1 \\ &= 0, & |\omega| > 1 \end{aligned} \tag{10}$$

where $f(\omega)$ denotes the vibrational frequency function with the neutron "frequency" inserted instead of the vibrational one. For negative frequencies $f(\omega)$ is defined as follows

$$f(-\omega) = f(\omega) \tag{11}$$

and normalized to unity[1]

$$\int_0^1 f(\omega)\,d\omega = 1 \tag{11}$$

$\gamma(0)$ is related to the Debye-Waller function by

$$2\,W = \frac{\hbar\,\varkappa^2}{2\,M}\,\gamma(0) \tag{12}$$

---

[1] ω is here measured in units of the maximum vibrational frequency $\omega_m = 4.1 \cdot 10^{13}\ \text{sec}^{-1}$.

and is introduced to normalize $g(\omega)$ as follows

$$\int_{-1}^{1} g(\omega)\, d\omega = 1. \tag{13}$$

On very general grounds we may conclude that $f(\omega)$ is everywhere continuous whereas $df/d\omega$ has a certain number of discontinuities [21, 22, 23], the strongest ones being of the following type:

$$\begin{aligned} f(\omega) &= |\omega - \omega_0|^{\frac{1}{2}}, & \omega &> \omega_c \\ &= 0, & \omega &< \omega_c \end{aligned} \tag{14}$$

$g(\omega)$ is shown in Fig. 5.

VII. Results on the scattering surfaces

The numerical results on the one-phonon scattering surfaces are presented in a series of figures. The direction of the incident neutrons is first along a principal axis of the crystal, and in Fig. 10 some results for different incident directions are given. By using full and dotted lines it has been possible to give an indication of the variation of the intensities in the same figures, dividing the strength into three classes:

$0 - 3\ 10^{-2}$ barns/steradian. cell: weak intensity
$3 - 15\ 10^{-2}$ barns/steradian. cell: medium intensity
$> 15\ 10^{-2}$ barns/steradian. cell: strong intensity.

The concentric circles, indicating the lengths of the neutron wave vectors, are drawn to make a reading off easier and they are labelled both by the corresponding vibrational frequency ω, measured in units of 10^{12} sec^{-1}, and by the corresponding neutron energy $\hbar^2 k^2/2m$. It must be noted that the intensities are very approximate. However, they give an idea of the variation with the scattering angle.

Fig. 6, $k_0 = 4.0 \cdot 10^8$ cm^{-1} ($\lambda = 1.57$ Å): Fig. (6 a) shows the scattering lines and Fig. (6 b) shows the intensities in more detail for the most intense lines. To indicate which curve in (b) belongs to a certain line in (a), the corresponding curves in the two figures are labelled by the same letter. The strong elastic peak corresponds to the incoherent zero-phonon scattering. The Laue scattering conditions are nearly fulfilled in certain directions and in (b) we see how the intensity increases when approaching a Bragg scattering angle.

Fig. 7, $k_0 = 3.0 \cdot 10^8$ cm^{-1} ($\lambda = 2.09$ Å): Especially the scattering lines representing phonon emission have been changed considerably compared with those in Fig. 6. Closed curves have been developed and by drawing the tangents of these from the footpoint of the incident wave vector we can construct the singular points defined by the vanishing of $|1 + \varepsilon\,(\mathbf{n} \cdot \mathbf{c}_s)/v|$.

Fig. 8, $k_0 = 1.8 \cdot 10^8$ cm^{-1} ($\lambda = 3.49$ Å): No indication of the intensity is given. Note how the scattering surfaces for phonon emission disappear when the neutron energy decreases. At the same time the remaining surfaces are more separated from each other and the variation of the neutron energy with the scattering angle is more obvious.

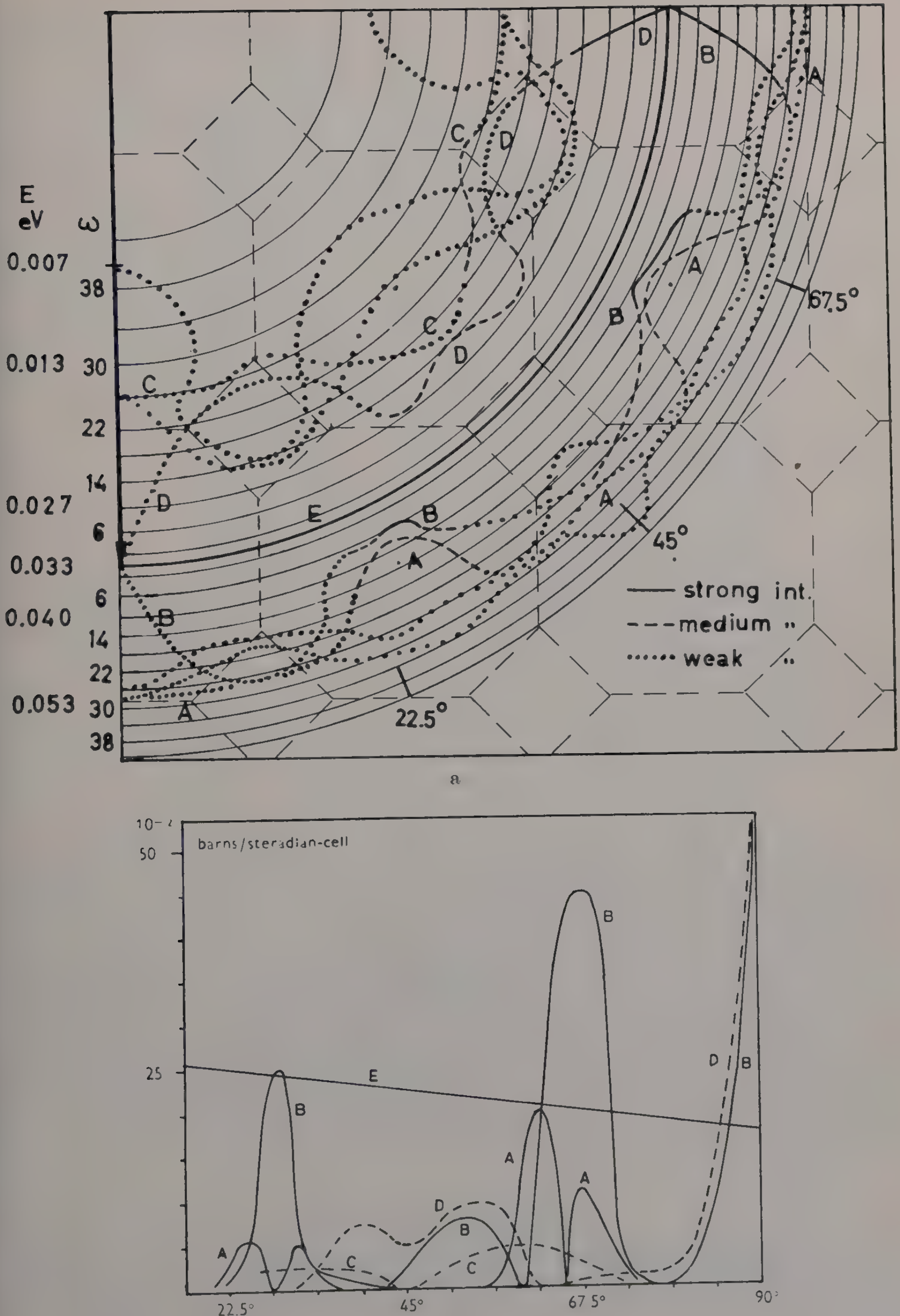

a

b

Fig. 6. $k_0 = 4.0 \cdot 10^8$ cm^{-1} ($\lambda = 1.57$ Å).

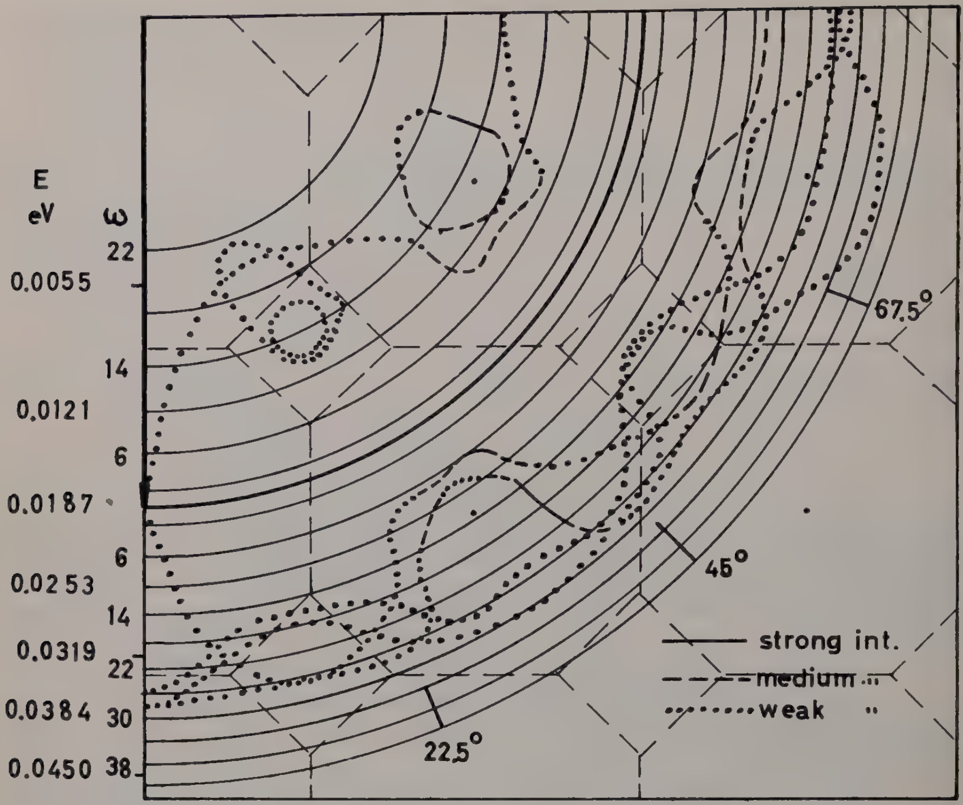

Fig. 7. $k_0 = 3.0 \cdot 10^8$ cm^{-1} ($\lambda = 2.09$ Å).

Fig. 9, $k_0 = 0$ ($\lambda = \infty$): For cold neutrons the wave length is large and then the scattering surfaces are approximately the same as those for infinite wave length. The intensity tends to infinity as $1/k_0$.

Fig. 10, $k_0 = 4.0 \cdot 10^8$ cm^{-1} ($\lambda = 1.57$ Å): The direction of $\mathbf{k}_0$ is varied in a principal plane, and it is shown how the scattering surfaces are altered within a certain reciprocal cell when passing a lattice point. To make Fig. (a) clearer the lines corresponding to ω_1 and ω_2 are drawn in separate cells. The angle between a principal axis and $\mathbf{k}_0$ is indicated and thus the lines for 0° correspond to those in Fig. 6a. In (b) more detailed results are given for the ω_1-lines, including an indication of the intensity. The factor $|1 + \varepsilon\ (\mathbf{n} \cdot \mathbf{c}_s)/v|$ has then been excluded and therefore the real intensity is appreciably increased when approaching a singular point.

ACKNOWLEDGEMENTS

I wish to express my gratitude to Professor I. Waller for suggesting this investigation. Special thanks are also due to Mr. E. Tenerz, who not only put his numerical material on KCl at my disposal but also guided me in its use and allowed me to publish some results on the eigen fre-

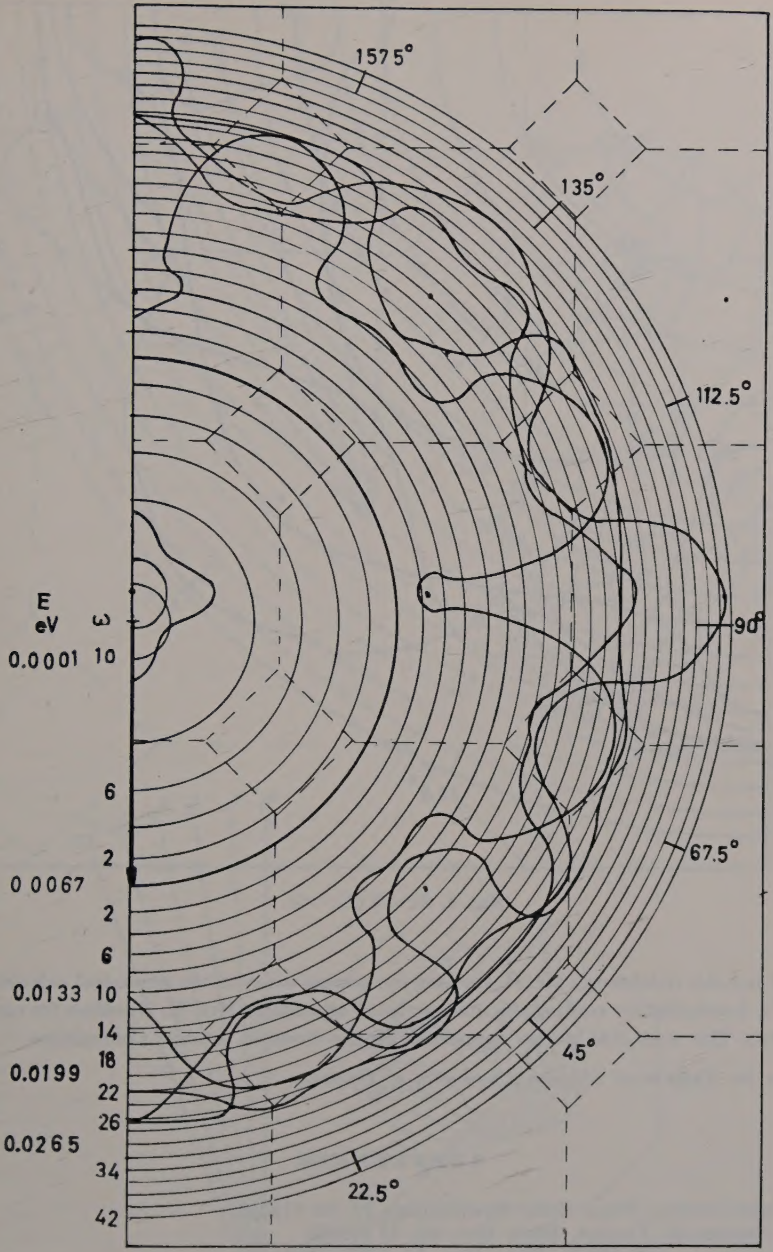

Fig. 8. $k_0 = 1.8 \cdot 10^8$ cm^{-1} ($\lambda = 3.49$ Å).

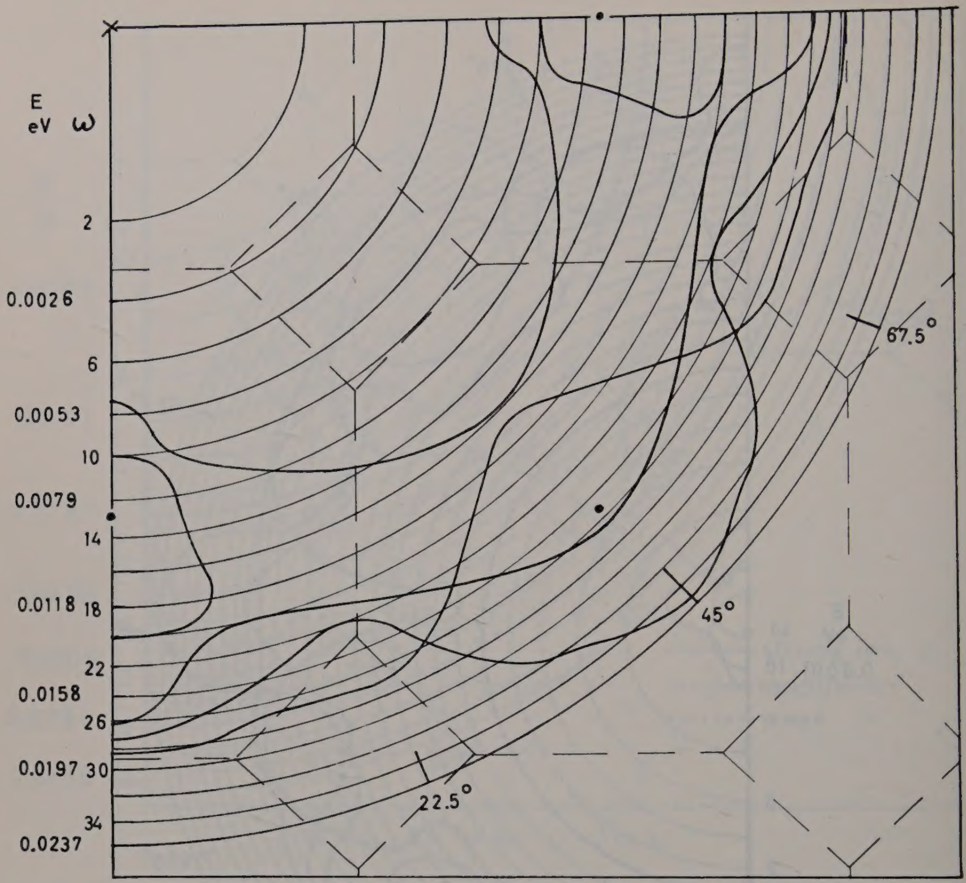

Fig. 9. $k_0 = 0$ ($\lambda = \infty$).

quencies. I am also indebted to Mr. H. Larsson for helping me with the numerical calculations and to Dr. S. O. Lundquist for reading the manuscript. I also thank Mrs. M. Nordfors for revising the English text. The work was partly supported by the Swedish Atomic Commission.

Institute for Theoretical Physics, University of Uppsala.

REFERENCES

1. I. Pomeranchuk, Phys. Zeits. Sowjetunion *13*, 65 (1938).
2. R. J. Seeger–E. Teller, Phys. Rev. *62*, 37 (1942).
3. G. Placzek–L. Van Hove, Phys. Rev. *93*, 1207 (1954).
4. R. S. Carter, D. J. Hughes, H. Palevsky, Phys. Rev. *99*, 611 (1955).
5. B. Jacrot, Compt. Rend. *240*, 745 (1955).
6. B. N. Brockhouse, A. T. Stewart, Phys. Rev. *100*, 756 (1955).
7. —— to appear in Rev. Mod. Phys., private communication.
8. R. S. Carter, H. R. Muether, D. J. Hughes, H. Palevsky, Bull. Am. Phys. Soc., Ser. II, *1*, 55 (1956).

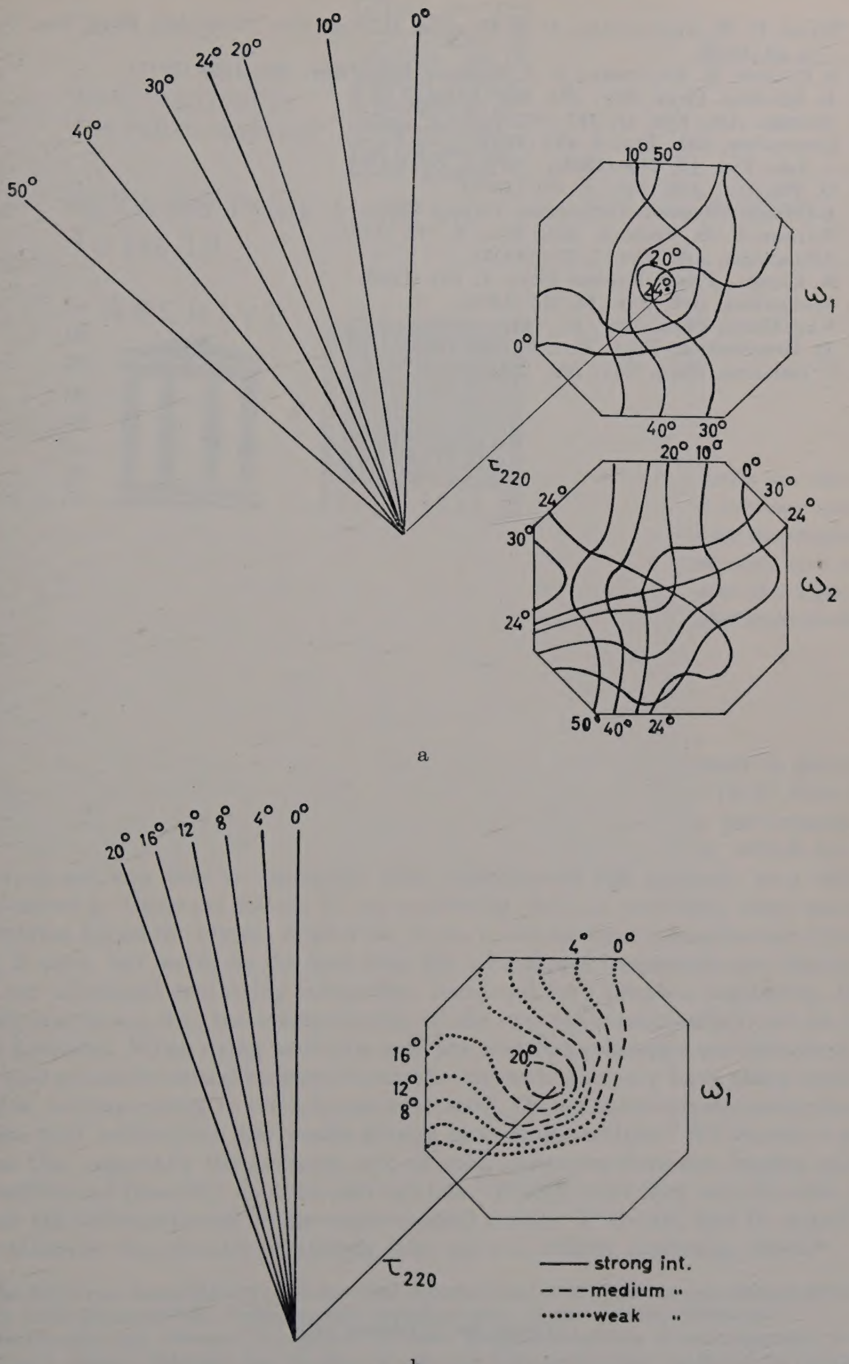

a

b

Fig. 10. $k_0 = 4.0 \cdot 10^8$ cm^{-1} ($\lambda = 1.57$ Å).

9. I. Pelah, C. M. Eisenhauer, D. J. Hughes, H. Palevsky, Bull. Am. Phys. Soc., Ser. II, *2*, 43 (1956).
10. R. S. Carter, H. Palevsky, D. J. Hughes, Phys. Rev. *106*, 1168 (1957).
11. G. L. Squires, Phys. Rev. *103*, 304 (1956).
12. E. Tenerz, Ark. Fys. *12*, 277 (1957).
13. S. Lundquist, Ark. Fys. *9*, 435 (1955).
14. —— Ark. Fys. *12*, 263 (1957).
15. P. O. Fröman, Ark. Fys. *4*, 191 (1951).
16. G. E. Bacon, Neutron Diffraction, Oxford 1955.
17. I. Waller–P. O. Fröman, Ark. Fys. *4*, 183 (1951).
18. A. Sjölander, Ark. Fys. *7*, 375 (1953).
19. J. M. Cassel, Progr. Nuclear Phys. *1*, 185 (1950).
20. A. Sjölander, Ark. Fys. *13*, 215 (1958).
21. L. Van Hove, Phys. Rev. *89*, 1189 (1953).
22. H. B. Rosenstock, Phys. Rev. *97*, 290 (1955).
23. J. C. Phillips, Phys. Rev. *104*, 1263 (1956).

Tryckt den 21 februari 1958

Uppsala 1958. Almqvist & Wiksells Boktryckeri AB